forests

MDPI

Article

Development of a Tree Growth Difference Equation and Its Application in Forecasting the Biomass Carbon Stocks of Chinese Forests in 2050

Hanyue Zhang, Zhongke Feng *, Panpan Chen and Xiaofeng Chen

Precision Forestry Key Laboratory of Beijing, Beijing Forestry University, Tsinghua East Road,
Beijing 100083, China
* Correspondence: zhongkefeng@bjfu.edu.cn; Tel.: +86-138-1030-5579

Received: 5 June 2019; Accepted: 11 July 2019; Published: 12 July 2019

Abstract: Global climate change has raised concerns about the relationship between ecosystems and forests, which is a core component of the carbon cycle and a critical factor in understanding and mitigating the effects of climate change. Forest models and sufficient information for predictions are important for ensuring efficient afforestation activities and sustainable forest development. Based on the theory of difference equations and the general rules of tree growth, this study established a difference equation for the relationship between the ratio of tree diameter at breast height (DBH) to the tree height and age of age of China's main arbor species. A comparison with equations that represent the traditional tree growth models, i.e., Logistic and Richards equations, showed that the difference equations exhibited higher precision for both fitting and verification data. Moreover, the biomass carbon stocks (BCS) of Chinese forests from 2013 to 2050 were predicted by combining the 8th Chinese Ministry of Forestry and partial continuous forest inventory (CFI) data sets. The results showed that the BCS of Chinese forests would increase from 7342 to 11,030 terra grams of carbon (Tg C) in 2013–2050, with an annual biomass C (carbon) sink of 99.68 Tg C year^{-1}, and they indicated that the Chinese land-surface forest vegetation has an important carbon sequestration capability.

Keywords: growth difference equation; growth prediction; biomass carbon stocks (BCS); Chinese forest

1. Introduction

As the "lung of the earth", forests are the material and spiritual basis for human survival and promote circulation of the ecosystem. Regardless of their geographical locations, they play an important role in climate changes such as precipitation, temperature, nitrogen and sulfur deposition, and carbon dioxide fixation [1,2]. Climate policy and the role of forests in reducing global warming have been important research agendas since the 1990s [3]. The potentially important role of carbon sinks has been recognized by the Kyoto Protocol of the Framework Convention on Climate Change, which includes carbon sequestration in the calculation of a country's net carbon emissions [4]. Only approximately half of the carbon dioxide emitted by fossil fuel combustion and deforestation accumulates in the atmosphere, and the remainder is found in the oceans and the terrestrial biosphere [5]. Uptake of net carbon by terrestrial ecosystems from the atmosphere plays a key role in slowing global warming in the global carbon cycle, and a large part of this absorption is due to forest ecosystems, which account for 30% of the land area [6,7]. Therefore, forest resource management is a concern of researchers in a broad range of fields, including forestry, economics, ecology, and other industries.

The vitality of trees is among the most important indicators of forest conditions and illuminates the dynamics of forest systems [8]. In these cases, the individual tree growth model is expected to replace the yield table as an appropriate aid for management decisions [9,10]. From a management perspective, effective, efficient, long-term, and sustainable forest management relies on useful and reliable information, such as the self-thinning rule and stand density index as well as models of existing and future forest conditions [11–13]. Growth and yield models have been and continue to be an important part of forestry research, and growth models are the most important components of long-term forest planning systems [14,15].

Empirical and theoretical equations have been applied mainly to study the population growth of trees, and their differential forms (i.e., the growth status at a certain time) are relatively complex. Difference equations, which reflect one of the essential properties of the real world, occupy an important place in mathematics and in real-world applications due to their discreteness, and these equations open up new approaches in solving one of the central problems of modern science, namely, the problem of turbulence [16]. The difference equation and discrete expression of differential equations belong to the field of nonlinear analysis in mathematics and can elucidate highly complex properties through a simple defined recursive relationship [17–19]. The theory of difference equations arises from the modeling of many aspects, including system theory, economics, inventory analysis, learning probability models, population genetics, and so on [20,21]. The theory of difference equations has been used in forestry and has shown a great advantage despite the fact that these equations have not been widely applied [22].

Up to 2010, China's forests constituted 5% of the global total and included a variety of forest biomes ranging from boreal forests in the north to subtropical/tropical evergreen broadleaf forests in the south [23,24]. Research on the growth of forest trees in China and their volumes, biomasses, and carbon stocks has attracted an increasing amount of attention. The tree diameter at breast height (DBH) and tree height are two important tree measurement factors that provide indispensable data for volume calculations and tree growth and harvest estimations [25]. Natural environmental factors and the spatial structure of forest stands affect the growth of trees. Weather, including precipitation and the average air temperature, also affects tree growth, but its effect is small, and the sizes and ages of tree species have a significantly greater impact on tree growth than do climatic variables [26–28]. Based on the general rule of the difference equation and tree growth, including certain empirical and theoretical, equations such as those of Schumacher (1939), the Logistic equation (1838), and Richards (1959) [29], this study proposed a new tree growth difference equation. The main feature of this equation is that it evaluates the relationship between the ratio of DBH and tree height with tree age. We tested and applied this differential equation considering the following aspects:

(1) Selection of 80% of the data to fit the model and use of the remaining 20% to validate the precision;
(2) Partial use of continuous forest inventory (CFI) data to test the practicability of the model;
(3) Combining data from the 8th Chinese Ministry of Forestry and CFI data sets to predict the growth status and biomass carbon stocks (BCS) of Chinese forests from 2013 to 2050.

2. Materials and Methods

2.1. Data

More than 120 tree species were obtained via analysis of the analytical wood data from "China's main tree growth compilation", which was compiled by the forestry survey team and other related units. These data were obtained by analyzing harvested trees. The DBH, size without bark and tree height were actual measured values. According to the 8th Chinese Ministry of Forestry data sets, China is extremely rich in tree species resources, with more than 8000 species of woody plants that account for approximately 54% of the world's resources. The woody plants in China include more than 2000 arbor trees. According to the dominant tree species statistics (groups), the top 10 tree genera and species are *Quercus* spp., *Betula* spp., *Cunninghamia lanceolate* (Lamb.) Hook., *Larix* spp., *Pinus massoniana* Lamb., *Populus* L., *Pinus yunnanensis* Franch., *Eucalyptus robusta* Smith, *Picea* spp., and *Cupressus* spp. These forests occupy 86.49 million hectares, accounting for 52.54% of the country's area, and their total accumulation of 7.015 billion cubic meters accounts for 47.47% of the country's area.

This study mainly investigated the dominant tree species in China according to the proportions of the main tree species groups and constructed a growth difference equation model for more than 10 tree species (groups), including *Quercus* spp., *Betula platyphylla* Suk., *Cunninghamia lanceolate* (Lamb.) Hook., *Larix* spp., *Pinus massoniana* Lamb., *Populus* L., *Pinus yunnanensis*, *Picea* spp., and *Pinus tabuliformis* Carrière. Due to the difficulties of early investigative work, the essential data for each species were taken from some of the main growth distribution areas. For example, the *Quercus* spp., *Betula platyphylla* Suk., *Populus* L., *Pinus tabuliformis* Carrière, and *Larix principis-rupprechtii* Mayr data are primarily from the Shanxi Province; the *Picea likiangensis* (Franch) Pritz, *Pinus yunnanensis* Franch., and *Abies georgei* Orr data are primarily from the Yunnan Province; the *Pinus massoniana* Lamb. data are mainly from the Sichuan Province; the *Abies fabri* (Mast.) Craib data are mainly from the Gansu and Shanxi Provinces; the *Larix gmelinii* (Ruprecht) Kuzeneva data are primarily from Inner Mongolia; and those for *Cunninghamia lanceolata* are primarily from the Fujian, Jiangxi, Anhui, and Hunan Provinces and other areas in South China. A database was established for each tree species, with the information shown in Table 1 and the area is shown in Figure 1.

Table 1. Model establishment and testing data for different tree species.

Location (Province/Autonomous Region)	Species		Number	Ranges		
				DBH (cm)	Height (m)	Age (year)
Sichuan	*Pinus massoniana* Lamb.		44	0.35–59.27	0.3–40.09	5–112
Sichuan, Gansu	*Abies fabri* (Mast.) Craib		16	0.25–45.9	0.11–27.3	5–161
Shandong	*Platycladus orientalis* (L.) Franco		9	0.3–39.6	0.3–16.06	5–264
Jiangxi, Fujian, Hunan, Guizhou, Anhui	*Cunninghamia lanceolate* (Lamb.) Hook.		388	0.35–42.95	0.3–30.5	5–106
Inner Mongolia	*Larix gmelinii* (Rupr.) Kuzen		44	0.5–36.7	0.3–31.8	5–210
Shanxi	*Larix principis-rupprechtii* Mayr		71	0.13–25.82	0.22–17.8	5–56
	Pinus tabuliformis Carrière		230	0.3–17.03	0.2–11	10–79
	Betula platyphylla Suk.		75	0.03–23	0.2–13.2	5–80
	Populus davidiana Dode		38	0.38–35.75	0.21–26.5	5–151
	Populus L.		31	0.3–21.9	1–14.7	5–104
	Picea spp.	*Picae asperata*	48	0.25–30.3	0.3–14.7	5–104
		Picea meyeri Rehd. et Wils	91	0.2–23.9	0.3–13.5	5–107
		Picea wilsonii Mast	18	0.2–43.75	0.3–19.05	5–195
	Quercus spp.	*Quercus aliena* Bl	11	0.3–23.8	0.4–18.5	5–79
		Quercus dentata Thunb	19	0.5–20.8	0.5–15.1	5–66
		Quercus wutaishansea Mary	22	0.4–37.3	0.6–31.3	5–85
Yunnan	*Picea likiangensis* (Franch) Pritz		49	0.8–88.8	0.5–52.7	10–349
	Pinus yunnanensis Franch.		48	1.5–55.5	0.63–38.8	5–149
	Abies georgei Orr		55	0.3–50	0.2–28.1	10–342

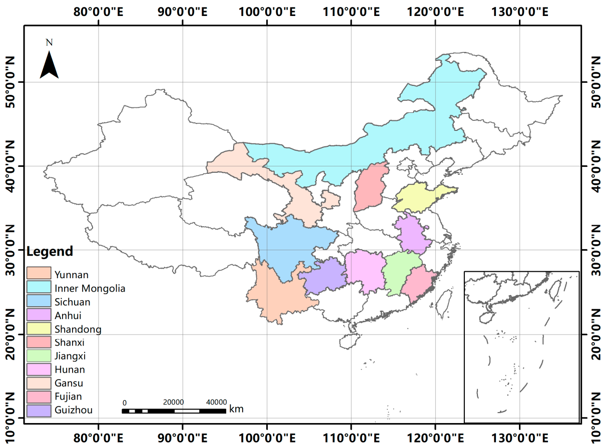

Figure 1. Distribution areas for model establishment and testing data for different tree species.

In the absence of a true external data set, the best method of validating the predictive ability of a model is to perform a statistical external validation, where the overall data set is divided into training and test data sets [30]. To test the applicability of the model and improve its application, 20% of our wood independent samples were used as testing sets to evaluate the model's precision. At the same time, we further validated and predicted China's carbon stocks in 2020, 2030, and 2050 using the National Forest Inventory (NFI) data, which were collected regularly at five-year intervals from 1999–2003, 2004–2008, and 2009–2013 [31]. In this study, the tree ages were calculated according to the DBH difference equation based on the 1999–2003 and 2004–2008 data, and the precision was tested by using actual and estimated values from 2009–2013. Finally, the carbon stocks in 2020, 2030, and 2050 were predicted and analyzed using NIF data from 2013 and the 8th Chinese Ministry of Forestry data.

2.2. Model Construction

The main empirical and theoretical equations for traditional tree growth, i.e., the Schumacher (1939), Korf (1939), Logistic (1838), and Richards (1959) equations, are primarily used to study the total growth process curve of tree growth [29]. Since the site conditions, environmental factors, stand conditions, and remote sensing information for the same tree will not change or will only change very slightly over a certain period of time except for during natural disasters, the influence of external environmental factors can be regarded as a fixed value k [27]. A difference equation is an equation that recursively defines a sequence, and each item of the sequence is a function defined as the previous item [32]. To predict the growth trend of trees over a certain period of time according to the general rule that tree growth is irreversible and slows as trees age, the DBH, tree height and age are taken into account to construct difference equations for the main tree species in China. The model is as follows:

$$\mathrm{k}\cdot Y_{t+1} = \mathrm{k}\cdot Y_t \cdot e^{b/t} + \mathrm{k}\cdot \varepsilon_{\mathrm{t}},\ \text{or}\ Y_{t+1} = Y_t \cdot e^{b/t} + \varepsilon_t, \tag{1}$$

Equation (1) can be extended to (2) as follows:

$$Y_{t+n} = Y_t \cdot e^{b/t} \cdot e^{b/t+1} \cdot e^{b/t+n-1} + \varepsilon_n, \tag{2}$$

where t is the tree age at the time of the investigation, Y_t is the DBH or tree height at the time of the investigation, Y_{t+1} is the DBH/tree height for the next year, Y_{t+n} is the DBH or tree height for the future nth year to be predicted, and b is the model coefficient.

Generally, tree age is determined by cutting down the tree or coring with growth cones [33]. Cutting down trees not only involves a large amount of work in the field but is also not a renewable use of forest resources. Coring involves bringing in individuals outside of the research team, and improper treatment may have a certain impact on tree growth. To determine the ages of trees, previous studies have mainly used the DBH or tree height at a certain time [34]. In this study, the difference model determined by Equation (1) can be used to predict the tree age without cutting down or coring. Age estimation is mainly based on a comparison of the DBH growth of two periods. To some extent, using multiperiod data can improve the estimation precision, such as for Equation (3):

$$t = \frac{\mathrm{b}}{\ln \frac{Y_{t+1}}{Y_t}}. \tag{3}$$

Equation (3) can be extended to (4) as follows:

$$\frac{1}{t} + \frac{1}{t+1} + \ldots + \frac{1}{t+n-1} = \frac{\ln Y_{t+n} - \ln Y_t}{\mathrm{b}}, \tag{4}$$

where t is the tree age at the time of the investigation, Y_t is the DBH/tree height at the time of the investigation, Y_{t+1} is the DBH or tree height for the next year, Y_{t+n} is the DBH or tree height of the future nth year to be predicted, and b is the model coefficient.

The Logistic equation was first used to describe population growth and is commonly used for simulating population dynamics in ecology. The curve is a typical symmetric "S" curve with initial values. The equation is as follows:

$$y = \frac{A}{1 + me^{-rt}}\ (A, m, r > 0), \tag{5}$$

where A is the maximum parameter value of tree growth, m is the parameter related to the initial value, and r is the intrinsic growth rate.

The Richards equation, which is based on the Von Bertalanffy growth theory and reflects the process of bio-energy assimilation and dissimilation, is widely used to describe the growth process of trees and has strong adaptability [28]. The equation is as follows:

$$y = A\left(1 - e^{-rt}\right)^c\ (A, r, c > 0), \tag{6}$$

where A is the maximum parameter value for tree growth, r is the growth rate parameter, and c is the parameter related to assimilation.

2.3. BCS Model

The mean biomass density, volume-derived, and remote sensing methods are three commonly used methods for estimating BCS [35]. The volume-derived method is considered to be the most effective and reliable method for forecasting BCS at large scales [36]. Therefore, this study employed the volume-derived method and used the NFI data to calculate China's forest volume M and its growth ΔM, which were calculated by the DBH-height model and the Chinese binary volume model, respectively, as shown in Equations (7)–(10). The parameters of the Chinese binary volume model are compiled by the Chinese agricultural department based on 197,000 samples of 180 tree species, and Cheng obtained the parameters of the DBH-height model tree model based on data consisting of 2082 samples. The specific parameters are shown in Table A1 [37].

$$\mathrm{M} = \sum\nolimits_1^j c_j \cdot \overline{d}_j^{\,g_j} \cdot \overline{H}_j^{\,f_j} \cdot \mathrm{N} \cdot k_j, \tag{7}$$

$$\Delta\mathrm{M} = \sum\nolimits_1^j c_j \cdot \left[\left(\overline{d}_j + \Delta d_j\right)^{g_j} \cdot \left(\overline{H}_j + \Delta H_j\right)^{f_j} - \overline{d}_j^{\,g_j} \cdot \overline{H}_j^{\,f_j}\right] \cdot \mathrm{N} \cdot k_j, \tag{8}$$

$$\Delta\mathrm{M} \approx \mathrm{M} \cdot \left(g_j \cdot \frac{\Delta d_j}{\overline{d}_j} + f_j \cdot \frac{\Delta H_j}{\overline{H}_j}\right), \tag{9}$$

$$\Delta\text{M} \approx \text{M}\cdot\frac{\Delta d_j}{\bar{d}_j}\cdot\left(g_j + f_j\cdot b_j\right), \tag{10}$$

where M is the forest volume; b_j, c_j, g_j, and f_j are model parameters for species *j*; k_j is the ratio of the tree species; N is the stand density; ΔM is the growth volume; Δd_j and ΔH_j are the growth of the DBH and tree height, respectively; and $\overline{d}_j$, and $\overline{H}_j$ are the average DBH and tree height, respectively.

According to the Chinese Ministry of Forestry, the average annual total wood loss from 1999 to 2013 was 4.342×10^8 m^3, which accounted for approximately 14.94% of the forest volume M. The values of growth rate c_j are shown in Table A1, and the gross growth of wood can be obtained from Equation (8). The wood consumption for each tree species was calculated proportionally to obtain the net increase. If forest biomass is calculated based on forest inventory data, then a biomass conversion factor (BEF) between biomass and stock volume must be established. The forest stand volume reflects the changes in forest age, site, forest density, and stand status [36]. To reflect the continuous changes of BEF, continuous variations of the conversion factor method were established to obtain the biomass and its growth component [38]. Qiu obtained the parameters of 41 tree species based on the 1607 fixed plot-point data according to Equations (11)–(12). The parameters are shown in Table A2 [39].

$$\text{B} = p_j\text{M} + q_j, \tag{11}$$

$$\Delta\text{B} = p_j\Delta\text{M}, \tag{12}$$

where M is the forest volume, ΔM is the growth volume, B is the biomass, ΔB is the growth part of the biomass, and p_j and q_j are model parameters for species *j*.

A certain proportional relationship exists between the BCS and biomass. Fang et al. [36] used a ratio of 0.5 to convert the biomass to C stocks. Saud et al. [40] assumed that species-specific gravity would help obtain the biomass and carbon stocks. Huang et al. [41] found that the carbon content of arbors ranges between 46.75% and 54.89% and averages 51.09%, and the parameters are shown in Table A3. The present study used different conversion factors to calculate the BCS and biomass C (carbon) sink according to Huang et al. as shown in Equations (13)–(14).

$$\text{C} = r_j\cdot\text{B}, \tag{13}$$

$$\Delta\text{C} = r_j\cdot\Delta\text{B}, \tag{14}$$

where C is the BCS, B is the biomass, ΔC is the biomass C sink, ΔB is the growth part of the biomass, and r_j is a model parameter for species *j*.

2.4. Model Evaluation and Validation

To validate the methodology introduced in the previous subsection, we examined the prediction accuracies achieved when estimating tree growth in terms of height h and diameter d. Typically, models use an independent dataset or data derived from data splitting or bootstrapping procedures. Huang et al. [42] provided a thorough review of these data selection methods and reported that independently collected data were the best test for a model. To evaluate the prediction performance and further test the applicability of these models, only 80% of the samples were randomly selected to establish the nonlinear function model in the form of Equation (2), which is evaluated by R^2, whereas the remaining 20% were used for model validation. This data selection method and ratio have been applied in many models, such as by Zeng et al., who developed individual tree crown biomass equations, and Cai et al., who developed accurate probabilistic models for important functional regions in DNA sequence through that [43,44]. The following goodness-of-fit statistics were used in the data evaluation: Residual (R), bias (BIAS), relative bias (BIAS%), mean absolute error (MAE), root mean square error (RMSE), relative root mean square error (RMSE%), empirical coefficient of correlation ($R^2{}_{\text{emp}}$), and Theil's inequality coefficient (U_2) [12,45]. BIAS was the difference between a population mean of the measurements or test results and an accepted reference or true value, MAE could explain the stability of model fitting, $R^2{}_{\text{emp}}$ could judge the model, and RMSE, BIAS%, RMSE%, and U_2 could reflect the precision of the model directly and clearly [46,47]. Their formulas are as follows:

R squared:

$$R^2 = 1 - (\text{residual sum of squares})/(\text{corrected sum of squares}). \tag{15}$$

Residual (*R*):

$$R = y_i - \hat{y}_i. \tag{16}$$

BIAS:

$$BIAS = \sum\nolimits_{i=1}^{n}\left(\frac{y_i - \hat{y}_i}{n}\right). \tag{17}$$

Relative bias (*BIAS*%):

$$BIAS\% = \frac{BIAS}{\overline{y}} \times 100. \tag{18}$$

Mean absolute error (*MAE*):

$$MAE = \sum\nolimits_{i=1}^{n}\left|\frac{y_i - \hat{y}_i}{n}\right|. \tag{19}$$

Root mean square error (*RMSE*):

$$RMSE = \sqrt{\frac{\sum_{i=1}^{n}(y_i - \hat{y}_i)^2}{n-1}}. \tag{20}$$

Relative root mean square error (*RMSE*%):

$$RMSE\% = \frac{\sqrt{\sum_{i=1}^{n}(y_i - \hat{y}_i)^2/n-1}}{\overline{y}} \cdot 100. \tag{21}$$

Empirical coefficient of correlation ($R^2{}_{\text{emp}}$):

$$R^2_{\text{emp}} = 1 - \left[\frac{\sum_{i=1}^{n}(y_i - \hat{y}_i)^2}{\sum_{i=1}^{n}(y_i - \overline{y})^2}\right]. \tag{22}$$

Theil's inequality coefficient U_2:

$$U_2 = \sqrt{\sum_{i=1}^{n}(y_i - \hat{y}_i)^2 \big/ \sum_{i=1}^{n}(y_i)^2}. \tag{23}$$

where y_i and $\hat{y}_i$ are the ith original observation and the predicted back-transformed value, respectively, n is the number of observations, and y is the mean of the observed values. All summations range from 1 to n.

3. Results

3.1. Growth Difference Equation

3.1.1. Model Fitting

To evaluate the influence of location factors such as longitude, latitude, temperature, and rainfall on tree growth, *Abies fabri* (Mast.) Craib in the Sichuan and Gansu Provinces and *Cunninghamia lanceolata* in the Jiangxi, Fujian, Hunan, Guizhou, and Anhui Provinces were analyzed. Due to the limited amount of data, 100% of the data were used to model each province. Equation (2) was estimated by nonlinear regression analysis and used the Marquardt iterative method to make the square sum convergence and parameters converge to 1×10^{-8} and obtain the parameter estimation and model fitting status with a 95% confidence interval. R^2, standard error (SE), and the parameter estimation results are shown in Table 2. The parameters of *Abies fabri* (Mast.) Craib showed no significant difference in the Sichuan and Gansu, and the results of *Cunninghamia lanceolata* also presented similar growth in five different provinces.

Table 2. Two-species growth difference equation to estimate differences between regions.

Species	Location	R^2	SE	Height (b)	R^2	SE	DBH (b)
Abies fabri (Mast.) Craib	Sichuan	0.986	0.065	1.174	0.986	0.069	1.273
	Gansu	0.994	0.032	1.231	0.99	0.04	1.409
Cunninghamia lanceolata	Jiangxi	0.945	0.009	0.8	0.906	0.012	0.78
	Fujian	0.947	0.02	0.808	0.933	0.027	0.867
	Hunan	0.938	0.024	0.806	0.906	0.031	0.906
	Guizhou	0.98	0.026	0.931	0.969	0.003	0.973
	Anhui	0.914	0.066	0.927	0.922	0.069	0.926

Note: In the equation $Y_{t+n} = Y_t{\cdot}e^{b/t}{\cdot}e^{b/t+1}\ldots\ldots{\cdot}e^{b/t+n-1}$. Y represents the DBH/tree height ratio; b is the parameter to be estimated; t is the year or age, and SE represents standard error.

We randomly selected 80% of all tree species for the modeling analysis, and 20% were selected for precision validation, except for *Platycladus orientalis* (L.) Franco, which was chosen for the k-fold cross-validation method due to the availability of fewer data sets. The results of the R^2 and SE to the model showed that the parameter of the model is reliable (Table 3). The parameter of *Picea* spp. (*Picea asperata*, *Picea meyeri* Rehd. et Wils, and *Picea wilsonii* Mast) in Shanxi did not significantly differ in the height or DBH models and the results of *Quercus* spp. (*Quercus aliena* Bl, *Quercus dentata* Thunb, and *Quercus wutaishansea* Mary) presented the same trend. The independence of observations is a fundamental assumption of ordinary least squares regression [17]. The estimated parameters are shown in Table 3.

Table 3. Growth difference equation of similar tree species in the same province.

Species	R^2	SE	Height (b)	R^2	SE	DBH (b)
Quercus aliena Bl	0.91	0.091	0.822	0.983	0.059	1.225
Quercus dentata Thunb	0.98	0.034	0.872	0.945	0.093	1.21
Quercus wutaishansea Mary	0.981	0.026	0.825	0.986	0.039	1.301
Picea asperata Mast.	0.977	0.032	1.568	0.885	0.077	1.949
Picea meyeri Rehd. et Wils	0.98	0.023	1.589	0.92	0.053	1.919
Picea wilsonii Mast	0.99	0.049	1.333	0.98	0.078	1.739

Note: In the equation $Y_{t+n} = Y_t{\cdot}e^{b/t}{\cdot}e^{b/t+1}\ldots\ldots{\cdot}e^{b/t+n-1}$. Y represents the DBH/tree height ration; b is the parameter to be estimated; and t is the year or age, and SE represents standard error.

The parameters of *Abies fabri* (Mast.) Craib in the Sichuan and Gansu province revealed no significant differences and that of *Cunninghamia lanceolata* in five different areas showed the similar results (shown in Table 2). In addition, the same tree genera such as the three species of *Picea* spp. in the Shanxi revealed no significant differences and that is similar to *Quercus spp.* in the Shanxi province (shown in Table 3). To improve the precision of the model and expand its applicability, the *Abies fabri* (Mast.) Craib data from the Sichuan and Gansu province were merged to establish a tree growth difference model suitable for a wider region and do the same processing for *Cunninghamia lanceolata* data from the Jiangxi, Fujian, Hunan, Guizhou, and Anhui provinces. A total of 80% of these data were randomly selected, and the remaining 20% were used to validate the precision and ensure the independence of the data. Meanwhile, other species were modeled and analyzed too. The estimated parameters and model indexes of Equations (1)–(4) for all tree species are shown in Table 4. Our results showed that the fitting determination coefficients (R^2) of the DBH difference model were all greater than 0.91 and that the R^2 of the tree height difference models were greater than 0.93, which indicates that the model could accurately represent the tree growth curve.

Table 4. Fitting results for the difference equation for different species.

Location	**Species (Groups)**	**Height**			**DBH**		
		R^2	**SE**	b	R^2	**SE**	b
Sichuan	*Pinus massoniana* Lamb.	0.969	0.025	0.823	0.984	0.025	1.008
Sichuan, Gansu	*Abies fabri* (Mast.) Craib	0.991	0.034	1.186	0.991	0.038	1.338
Shandong	*Platycladus orientalis* (L.) Franco	0.986	0.045	0.717	0.987	0.065	0.938
Jiangxi, Fujian, Hunan, Guizhou, Anhui	*Cunninghamia lanceolata*	0.952	0.009	0.82	0.93	0.001	0.829
Inner Mongolia	*Larix gmelinii* (Ruprecht) Kuzeneva	0.979	0.019	0.785	0.984	0.002	0.906
Shanxi	*Larix principis-rupprechtii* Mayr	0.949	0.032	1.348	0.918	0.045	1.578
	Picea spp.	0.984	0.018	1.527	0.94	0.038	1.889
	Quercus spp.	0.965	0.026	0.842	0.966	0.041	1.250
	Pinus tabuliformis Carrière	0.975	0.012	1.065	0.968	0.02	1.306
	Betula platyphylla Suk.	0.959	0.022	1.016	0.962	0.028	1.356
	Populus davidiana Dode	0.94	0.03	0.981	0.964	0.033	1.405
	Populus L.	0.951	0.03	0.728	0.956	0.034	1.008
Yunnan	*Picea likiangensis* (Franch) Pritz	0.994	0.015	0.885	0.995	0.015	0.842
	Pinus yunnanensis French.	0.939	0.022	0.758	0.966	0.019	0.729
	Abies georgei Orr	0.997	0.016	1.016	0.996	0.02	1.089

Note: In the equation $Y_{t+n} = Y_t \cdot e^{b/t} \cdot e^{b/t+1} \ldots\ldots \cdot e^{b/t+n-1}$ Y represents the DBH/tree height ration; b is the parameter to be estimated; and t is the year or age, and SE represents standard error. *Picea* spp. includes *Picea asperata*, *Picea meyeri* Rehd. et Wils, and *Picea wilsonii* Mast., *Quercus* spp., includes *Quercus aliena* Bl, *Quercus dentata* Thunb, and *Quercus wutaishansea* Mary.

To test the applicability of the difference equation, the Logistic and Richards equations (5)–(6) were applied separately to the same data; the results are shown in Tables A4 and A5. Significant differences were not observed between the R^2 values of the Logistic and Richards equations, and both can be effectively applied to most tree species; however, the equations cannot be applied to several species, such as *Populus* L., whose R^2 value was approximately 0.4.

3.1.2. Model Precision Evaluation Using the Testing Data

To obtain the prediction precision for the different modeled tree species, 20% of the samples were used for data validation. The evaluation employed BIAS, BIAS%, MAE, RMSE, RMSE%, R^2_{emp}, and U_2 as indicators for precision testing, and the results are shown in Tables 5 and 6.

In Table 5, height difference models for all species show that the BIAS values were all near 0; BIAS% and RMSE% were less than 5.49% and 11.45%, respectively; R^2_{emp} values were greater than 0.93; and most MAE values were less than 1. These results indicate that the models were relatively stable and could be used to predict the height growth. For the DBH difference model precision shown in Table 6, the BIAS% values were less than 5% except for those of *Abies fabri* (Mast.) Craib, *Picea* spp. and *Populus* L., and *Abies fabri* (Mast.) Craib was the highest, at 10.17%. The MAE values were mostly less than 1, and the maximum RMSE% value was 16.05%; the R^2 values were greater than 0.91 except for that of *Picea* spp., and the U_2 values were close to 0. These findings indicated that the model had high fitting stability and could achieve good prediction precision.

As with the difference equation, BIAS, MAE, RMSE, and R^2_{emp} were used to validate the Logistic and Richards equations for DBH and tree height. The results are shown in Tables A6 and A7. The precision of each tree height index was higher than the DBH precision, indicating that the equation was better suited to simulating tree height growth. The R^2_{emp} values of different species were significantly different, indicating that it could be applied to some species well but not to others.

Table 5. Validation precision of tree height difference equations for different tree species.

Species (Groups)	**BIAS (m)**	**BIAS%**	**MAE (m)**	**RMSE (m)**	**RMSE%**	**R^2_{emp}**	**U_2**
Pinus massoniana Lamb.	0.004	0.02	0.905	1.163	6.85	0.976	0.062
Abies fabri (Mast.) Craib	0.198	2.2	0.366	0.542	3.9	0.994	0.048
Platycladus orientalis (L.) Franco	−0.036	−0.411	0.317	0.410	4.88	0.993	0.043
Cunninghamia lanceolata	−0.042	−0.31	1.03	1.333	7.75	0.943	0.091
Larix gmelinii (Ruprecht) Kuzeneva	0.171	1.02	0.841	1.175	4.74	0.972	0.065
Larix principis-rupprechtii Mayr	0.096	1.3	0.657	0.83	11.24	0.961	0.097
Picea spp.	0.096	2.3	0.341	0.466	11.14	0.999	0.09
Quercus spp.	−0.096	−1.06	0.448	0.597	6.64	0.993	0.119
Pinus tabuliformis Carrière	0.128	2.193	0.452	0.670	11.45	0.952	0.101
Betula platyphylla Suk.	−0.164	−1.89	0.737	0.942	10.87	0.934	0.1
Populus davidiana	0.031	0.31	0.685	0.847	8.52	0.975	0.088
Populus L.	0.516	5.49	0.636	0.968	10.28	0.942	0.094
Picea likiangensis	−0.177	−0.72	0.669	0.848	3.48	0.995	0.031
Pinus yunnanensis	−0.342	−1.47	1.525	1.922	8.28	0.941	0.078
Abies georgei Orr	−0.075	−0.64	0.415	0.555	4.69	0.996	0.038

Table 6. Validation precision of the tree diameter at breast height (DBH) difference equations for different tree species.

Species (Groups)	**BIAS (cm)**	**BIAS%**	**MAE (cm)**	**RMSE (cm)**	**RMSE%**	**R^2_{emp}**	**U_2**
Pinus massoniana Lamb.	0.326	1.53	0.972	1.368	6.44	0.987	0.056
Abies fabri (Mast.) Craib	1.85	10.17	1.852	2.257	12.41	0.946	0.109
Platycladus orientalis (L.) Franco	0.164	0.920	0.689	0.891	4.994	0.991	0.044
Cunninghamia lanceolata	0.231	1.35	1.605	2.158	13.66	0.912	0.116
Larix gmelinii (Ruprecht) Kuzeneva	0.209	1.23	0.874	1.123	6.59	0.984	0.058
Larix principis-rupprechtii Mayr	0.347	3.59	0.923	1.167	12.1	0.944	0.107
Picea spp.	0.431	5.19	1.012	1.333	16.05	0.884	0.145
Quercus spp.	−0.059	−0.47	0.664	1.066	8.42	0.983	0.064
Pinus tabuliformis Carrière	0.442	4.90	0.807	1.073	11.88	0.954	0.104
Betula platyphylla Suk.	−0.262	−2.75	0.836	0.998	10.5	0.953	0.094
Populus davidiana	−0.159	−1.16	0.883	1.057	7.68	0.982	0.066
Populus L.	0.606	6.85	0.761	1.02	11.53	0.955	0.1
Picea likiangensis	−0.259	−0.75	1.031	1.335	3.84	0.993	0.035
Pinus yunnanensis	−0.603	−2.1	1.333	1.567	5.45	0.983	0.05
Abies georgei Orr	−0.086	−0.36	0.827	1.158	4.82	0.995	0.039

3.1.3. Model Precision Evaluation Using the CFI Data

To test the practicability of the model, this study used CFI data. Since the age of each tree could not be determined, Equation (4) was used to estimate these values. The DBH data investigated from 1999–2003 and 2004–2008 could be used to estimate the ages of the trees. These data were gathered from the province in which the model was built. At the same time, the estimated ages and the data from 2004–2008 were used to forecast the growth in 2009–2013 with Equation (2), with $n = 5$. The comparison between the predicted status and the actual true value is shown in Figure 1. The residual can be obtained from this equation and can be used to evaluate the uniformity and normality. The results showed that the residuals were distributed homogeneously, meaning that they had no heterogeneity, which conformed to the general law of error distribution [46].

The growth results obtained using the model estimation were regarded as predicted values, whereas those obtained by the actual measurements were seen as actual values. Figure 1 shows that the predicted value and the true value of each species were linearly fitted; the linear relationship is shown by the red line, and that the R^2 value was greater than 0.91. The R^2 values of some species, such as *Picea asperata* Mast (Figure 2g), *Quercus* spp. (Figure 2h), and *Picea likiangensis* (Figure 2l), reached 0.99, indicating that these values were linearly related, and the slope of each species was very close to 1, showing that the predicted and true values were not significantly different. In addition, *Larix gmelinii (Ruprecht) Kuzeneva* (Figure 2e) fell below the 1:1 line, which indicated that the overall prediction effect was less than the actual growth. All other species presented a fitting curve closer to the 1:1 line, especially *Pinus massoniana Lamb.* (Figure 2a), *Quercus spp.* (Figure 2h), and *Abies georgei Orr* (Figure 2n) et al.

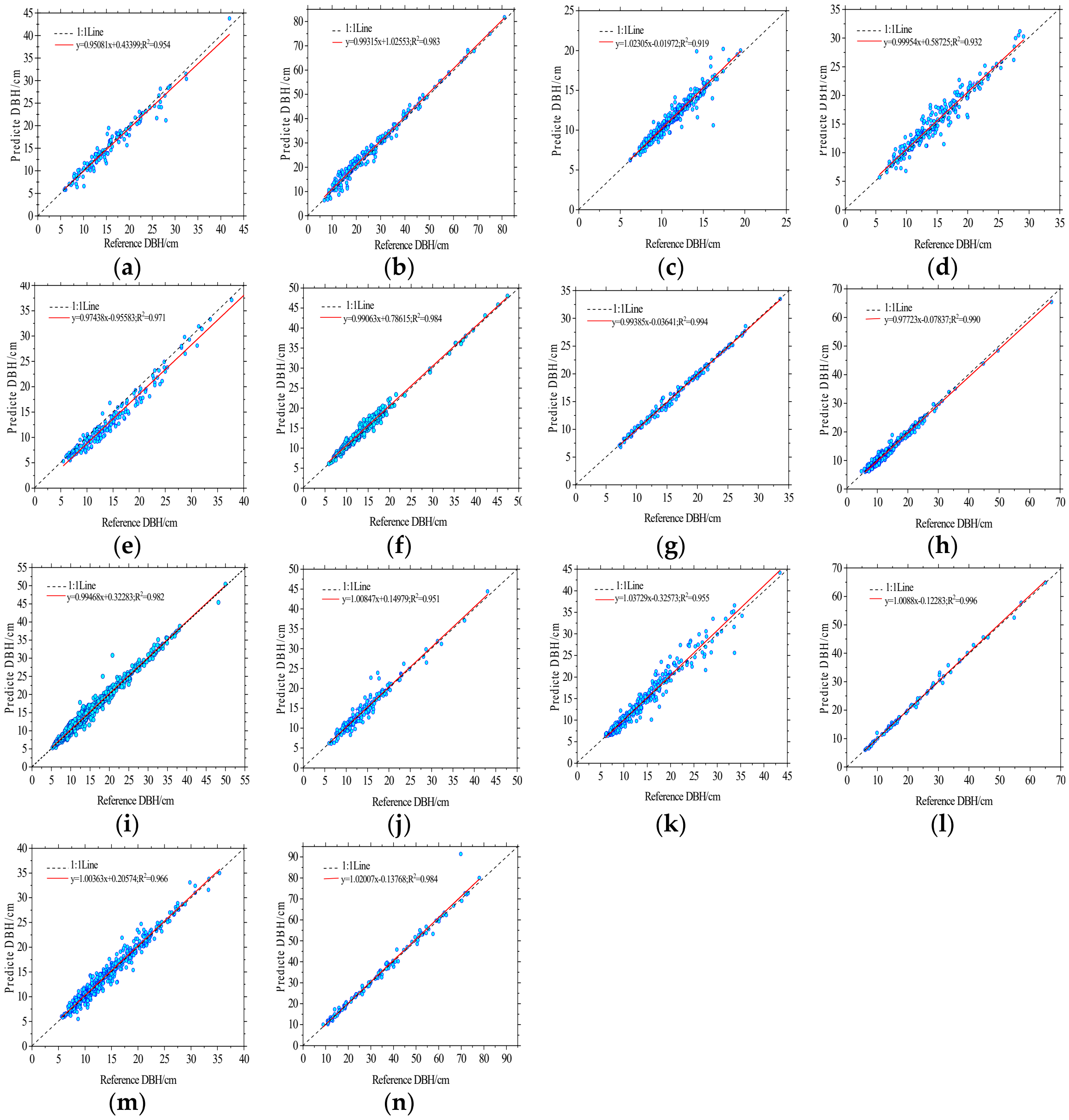

Figure 2. Fitting curve of the DBH between the predicted and actual values. The names of the tree species are as follows: (**a**): *Pinus massoniana* Lamb.; (**b**): *Abies fabri* (Mast.) Craib; (**c**): *Platycladus orientalis* (L.) Franco; (**d**): *Cunninghamia lanceolata*; (**e**): *Larix gmelinii* (Ruprecht) Kuzeneva; (**f**): *Larix principis-rupprechtii*; (**g**): *Picea asperata* Mast; (**h**): *Quercus* spp.; (**i**): *Pinus tabuliformis* Carrière; (**j**): *Betula platyphylla* Suk.; (**k**): *Populus* L.; (**l**): *Picea likiangensis*; (**m**): *Pinus yunnanensis*; and (**n**): *Abies georgei* Orr.

3.2. BCS Forecast for Chinese Forests in 2050

The forest volumes and their areas in 2013 can be obtained using the 8th Chinese Ministry of Forestry data sets. The difference equation was used to predict the DBH growth in China using continuous forest inventory (CFI) data, which were randomly and evenly distributed in various provinces of China. By combining the average DBH with the annual increase in DBH, volume, biomass and BCS in 2013, the increases in the volume, biomass, and BCS were predicted for 2050. The results are shown in Table 7.

Table 7. The volume and area of Chinese forests in 2013 and the annual increases in DBH, volume, biomass, and biomass carbon stocks (BCS) in 2013–2050.

Species (Groups)	M (10^8 m^3)	AREA (10^4 ha)	$\Delta\bar{d}$ (year^{-1}) (cm)	ΔM (year^{-1}) (10^8 m^3)	ΔB (year^{-1}) (Tg)	ΔC (year^{-1}) (Tg C)
Quercus spp.	12.94	146	0.3	0.23	21.92	10.59
Betula spp.	9.14	1112	0.2	0.15	12.03	5.94
Larix spp.	10.01	1070	0.24	0.16	15.01	7.89
Pinus massoniana Lamb.	5.91	1000	0.42	0.12	7.61	3.91
Pinus yunnanensis	4.77	410	0.25	0.08	5.85	3.09
Picea asperata Mast	9.87	385	0.24	0.16	7.5	3.87
Abies fabri (Mast.) Craib	11.65	308	0.24	0.18	9.53	4.81
Cupressus funebris Endl.	2	366	0.18	0.03	1.7	0.89
Cunninghamia lanceolata	7.26	1097	0.34	0.14	7.32	3.93
Populus L.	5.03	854	0.38	0.09	6.8	3.37
Pinus tabuliformis Carrière	0.66	161	0.31	0.01	0.94	0.5
Other species	68.53	8027	0.27	1.18	99.03	50.89
Total	147.77	14936	–	2.53	195.24	99.68

Note: M is the volume of each species, ΔM is the growth volume, $\Delta\bar{d}$ is the growth of the average DBH, ΔB is the growth part of the biomass, ΔC is the biomass C sink, year^{-1} represents annual growth, and Tg C represents terra gram of carbon.

Table 7 shows that the average growth rates for trees of each species were similar. The annual growth was approximately 0.2–0.4 cm in 2013–2050, *Cunninghamia lanceolate* (Lamb.) Hook. and *Populus* L. (up to 0.34 cm and 0.38 cm, respectively) had relatively high growth rates, and the growth rate of *Pinus massoniana* Lamb. was the highest, reaching at 0.42 cm. The area of *Quercus spp.* species was the smallest, but its volume, annual growth volume and biomass C sink were the largest. The highest biomass C sink was 10.61 Tg C·year^{-1} and the lowest was 0.37 Tg C·year^{-1}, which may be related to the volume of this species. From 2013 to 2050, the total growth of China's forests will increase by 2.53×10^8 m^3·year^{-1} and the BCS will increase by 99.68 Tg C·year^{-1}.

The natural growth and the consumption of timber resources resulted in a certain amount of wood loss per year. According to the wood loss ration of the annual total volume in 1999–2013, the total loss could be predicted, and timber harvesting shifted from earlier clear-cutting to include selective and staged cuttings, which did not change overall forest cover, thus, the loss of various tree species in 2013–2020, 2020–2030, and 2030–2050 was predicted according to their proportion in this study [48]. The DBH growth and the gross growth of timber volume could be predicted by the difference equations (Equation (2) and Equation (10)) in order to obtain the net increase. The results were shown in Table 8 and Figure 3, the volume and proportion of net growth to gross growth both increased (Figure 3).

Table 8. The gross growth, loss, and net increase of the volume of different tree species in Chinese forests from 2013 to 2050.

Species (Groups)	**2013–2020 (10^8 m^3)**			**2020–2030 (10^8 m^3)**			**2030–2050 (10^8 m^3)**		
	Growth	**Loss**	**Increase**	**Growth**	**Loss**	**Increase**	**Growth**	**Loss**	**Increase**
Quercus spp.	1.89	1.07	0.82	2.83	1.29	1.54	5.01	1.94	3.07
Betula spp.	2.22	1.31	0.91	3.29	1.58	1.71	5.76	2.34	3.42
Larix spp.	2.82	2.17	0.65	3.76	2.52	1.24	5.32	2.88	2.44
Pinus massoniana Lamb.	1.57	1.1	0.47	2.04	1.16	0.88	3.03	1.33	1.7
Pinus yunnanensis	1.8	0.94	0.86	2.79	1.16	1.63	5.31	2.02	3.29
Picea asperata Mast	1.77	0.78	0.99	3.1	1.2	1.9	5.68	1.92	3.76
Abies fabri (Mast.) Craib	0.41	0.23	0.18	0.59	0.26	0.33	1	0.35	0.65
Cupressus funebris Endl.	3.26	2.48	0.78	4.18	2.71	1.47	5.85	2.99	2.86
Cunninghamia lanceolata	2.04	1.52	0.52	2.76	1.76	1	4.03	2.06	1.97
Populus L.	0.22	0.15	0.07	0.32	0.19	0.13	0.52	0.27	0.25
Pinus tabuliformis Carrière	20.69	14.08	6.61	28.76	16.24	12.52	45.18	20.49	24.69
Other species	20.69	14.07	6.62	28.77	16.23	12.54	45.19	20.44	24.75

Note: Loss (mortality and cut) = total loss × (volume of the species/volume total).

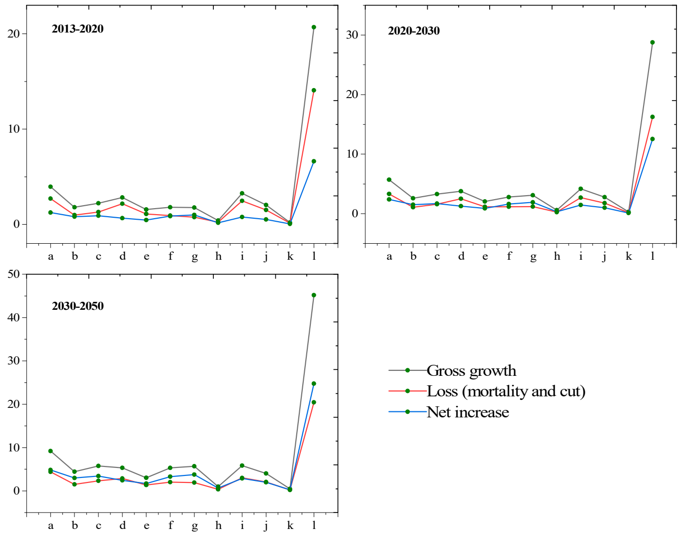

Figure 3. The gross growth, loss, and net increase of the volume of different tree species in Chinese forests from 2013 to 2050. Meaning of each letter: a: *Quercus* spp.; b: *Betula* spp.; c: *Larix* spp.; d: *Pinus massoniana* Lamb.; e: *Pinus yunnanensis*; f: *Picea asperata* Mast; g: *Abies fabri* (Mast.) Craib; h: *Cupressus funebris* Endl.; i: *Cunninghamia lanceolata*; j: *Populus* L.; k: *Pinus tabuliformis* Carrière; and l: *Other species*.

As shown in Table 9 and Figure 4, the average DBH values of all species in 2013 were in the middle diameter group, and most were 15 cm. *Picea asperata Mast* and *Abies fabri* (Mast.) Craib had DBH values of 19.26 and 21.64 cm, respectively, and the two species presented a relatively high growth (Table 9 and Figure 4I), indicating that small trees occupy a large proportion. Moreover, the volume, biomass, and carbon stock of all tree species will increase significantly and the accumulation of the species will not significantly differ between 2013 and 2050. By 2050, the timber volume (Table 9 and Figure 4II) will increase by 93.77×10^8 m^3, the biomass C sink (Table 9 and Figure 4IV) will reach 3688.05 Tg C and the carbon stock (Table 9 and Figure 4IV) will reach 11,030 Tg C, showing that Chinese forests will play an important role in carbon sequestration.

Table 9. DBH, volume, biomass, and BCS of Chinese forests in 2013 and 2050.

Species (Groups)	**D (cm)**		**M (10^8 m^3)**		**B (Tg)**		**BCS (Tg C)**	
	2013	**2050**	**2013**	**2050**	**2013**	**2050**	**2013**	**2050**
Quercus spp.	14.94	26.02	12.94	21.39	1305.1	2116.09	630.63	1022.49
Betula spp.	14.08	21.38	9.14	14.57	950.53	1395.6	469.37	689.15
Larix spp.	16.75	25.48	10.01	16.05	785.67	1341.1	413.18	705.29
Pinus massoniana Lamb.	15.25	30.67	5.91	10.24	641.76	923.19	330.12	474.89
Pinus yunnanensis	14.35	23.6	4.77	7.82	416.54	632.87	219.98	334.22
Picea asperata Mast	19.26	28.2	9.87	15.65	786.16	1063.64	405.66	548.84
Abies fabri (Mast.) Craib	21.64	30.54	11.65	18.3	688.14	1040.68	347.51	525.54
Cupressus funebris Endl.	14.27	20.79	2	3.16	279.46	342.34	145.62	178.39
Cunninghamia lanceolata	14.29	26.94	7.26	12.37	636.59	907.31	341.53	486.77
Populus L.	15.67	29.61	5.03	8.52	575.08	826.59	285.01	409.66
Pinus tabuliformis Carriifo	14.76	26.25	0.66	1.11	73.84	108.59	39.24	57.7
Other species	14.73	24.66	68.53	112.36	7227.59	10891.71	3714.2	5597.16

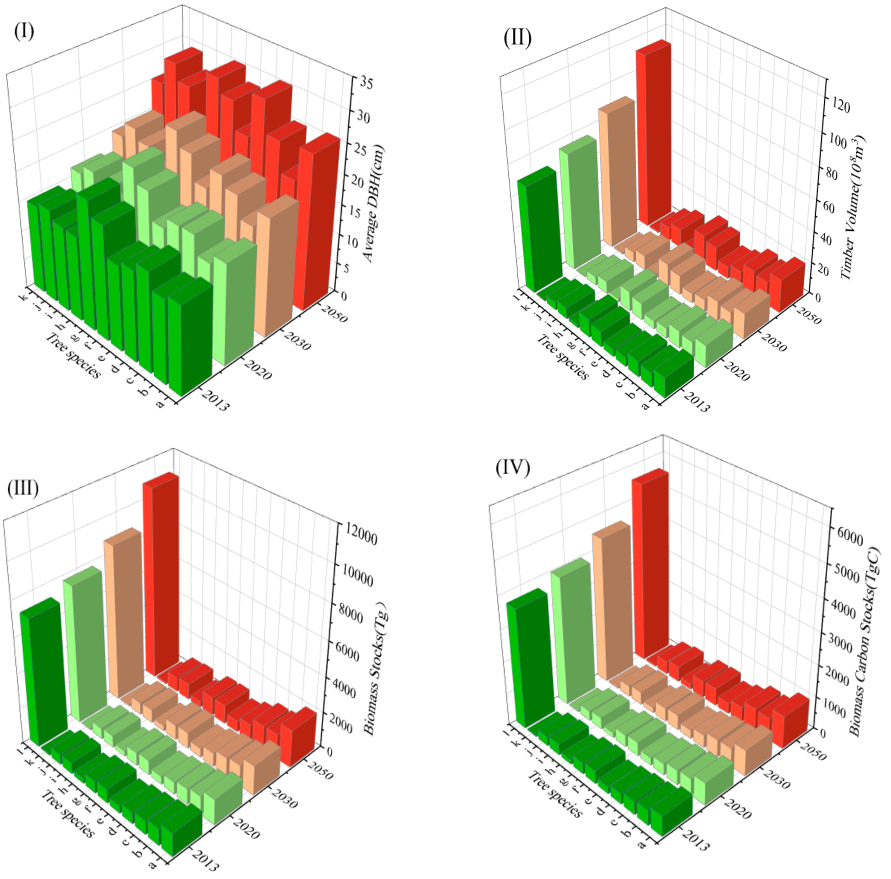

Figure 4. DBH, volume, biomass, and BCS of Chinese forests from 2013 to 2050. Meaning of each picture: (**I**): Average DBH; (**II**): Timber volume; (**III**): Biomass stocks; (**IV**): Biomass carbon stocks. Meaning of each letter: a: *Quercus* spp.; b: *Betula* spp.; c: *Larix* spp.; d: *Pinus massoniana* Lamb.; e: *Pinus yunnanensis*; f: *Picea asperata* Mast; g: *Abies fabri* (Mast.) Craib; h: *Cupressus funebris* Endl.; i: *Cunninghamia lanceolata*; j: *Populus* L.; k: *Pinus tabuliformis* Carrière; and l: *Other species*.

4. Discussion

4.1. Arbor Growth Difference Equation

Tree growth is an important facet of forest dynamics and can provide information on the health, productivity, and sustainability of a forest as well as the spatial and temporal variability in growth rates [49]. DBH and tree height growth models are considered to be effective projections of tree growth, and studies of tree growth models are the basis of forest research [15]. The DBH and tree height model fitting and precision validation data showed that the growth difference equation was adequate for these data.

Many scholars believe that validation is an important part of modeling, because validation precision can show the model's reliability [50]. Aggregating similar species into one species can increase the amount of modeling data and improve the fitting precision, and using the nonlinear function to fit the equation directly can avoid transformation bias [51,52]. Model efficiencies can commonly exceed 0.50 for distance-independent individual-tree diameter growth models fit for related forest types [53]. As important decision-making tools in forestry, individual-tree growth models have been the subject of considerable research, such as that by Schliep et al. [54], Lhotka et al. [55], Moreno et al. [12], etc. Schliep et al. [54] modeled individual tree growth by fusing diameter tape and increment core data. Lhotka et al. [55] developed an individual-tree model that presented R^2 values from 0.26 to 0.57, and better fit was observed for oak species based on a mixed-effects regression and 290 inventory plots. Moreno et al. [12] used the AIDBH model with the cross-validation (CV) and LASSO regression selection variable procedures and found that the $R^2{}_{\text{emp}}$ of annual DBH growth predictions was 0.56 and DBH projections at six and 12 years 0.98 and 0.97, respectively. The model structure represented by the form of the difference equation is convenient and easy to use for such applications [53]. In this study, the difference equation for the relationship between the DBH/tree height ratio and tree age was an individual-tree growth model, which was developed for China's main arbor species. The fitting R^2 values and validation $R^2{}_{\text{emp}}$ values for this model were greater than 0.91 and the BIAS, MAE, RMSE, and U_2 values were relatively small, indicating the goodness-of-fit of the model. Although some deviations were observed in certain data predictions, these deviations could be due to the heterogeneity of the growth environments, measurement errors, or model shortcomings. The influence of different tree shapes and the growth environment (water, nutrients, light, crown and root space, etc.), which is seen as a fixed value, has been reflected by the difference in the DBH and height at the same age. Additionally, the model assumes that the growth environment of an individual tree will not change suddenly and thus can be expanded for use. Meanwhile, comparing the fitting and validation precision among the Logistic, Richards, and difference equations based on the same data set reveals that the difference equation had a higher precision than the Logistic and Richards equations for tree height and DBH. This phenomenon may occur because the difference equation was predicted based on the DBH or tree height of a certain year, which contained information related to the growth environment/site conditions, etc. Therefore, the difference equation had a remarkable parameter estimation effect and could obtain higher precision for rapid, simple, and efficient tree growth predictions.

Difference equations have been applied in forestry research [22,56]. Kiviste et al. [56] constructed an algebraic difference model to explore the relationship between stand height, diameter, and volume growth with the present state of stand description data. Faster and slower growth rates are biological phenomena, and tree growth is affected by several biotic and abiotic factors [19,57]. In this study, the difference equation parameters showed that tree growth was less affected by the spatial positioning of the tree species. A certain similarity was observed among different tree species in the same group that grow in the same region, and the growth rates of different tree species were significantly different. All of these findings indicated that external factors, such as the environmental climate and stand density, had few influences, whereas internal factors, such as the tree species, age and size, were the main reasons for tree growth. Relevant studies also showed that tree growth reacted dynamically to climate change with aging, which is a continuous process [58,59]. Therefore, an important relationship occurs between studies of tree growth and the ecological environment and climate, and numerous studies remain to be performed.

4.2. BCS Forecast for Chinese Forests

Forests play an important role in regional and global carbon cycles. The long history of agricultural exploitation, forest management practice, and changing land use and forestry policies suggests that Chinese forests are vital. Recently, many scholars have conducted extensive research on BCS in various countries [36,60–63]. Research on China's forest carbon stocks has received extensive attention, and many scholars have studied China's carbon resources for several years. For the 1973–1976, 1977–1981, 1984–1988, and 1989–1993 periods, Fang et al. [36] estimated the BCS of forest stands in China to be 4440, 4380, 4450, and 4630 Tg C, respectively, with the continuous biomass expansion factor (CBEF) method, whereas the estimates of Pan et al. [62] were 3510, 3600, 3690, and 4020 Tg C, respectively, with an age-specific CBEF method. Fang et al. [38] and Guo et al. [63] estimated values of 5010 and 5850 Tg C for the periods from 1994–1998 and 1999–2003, respectively, with the CBEF method. Zhang et al. [35] estimated an increase from 4110 to 6240 Tg C and reported that the BCS of all types of forests in China increased from 4930 to 8120 Tg C from 1973 to 2008.

Inventory-based estimation of BCS of forests at both regional and national scales may help to reduce the uncertainties in accurately evaluating the role of forests in regional and global C budgets [34]. In this study, the difference equation was used to predict the DBH of trees and then to predict increases in the volume, biomass, and BCS. Losses caused by forest fires, pests, wood harvesting, and other human activities were considered. Thus, from 2013 to 2050, we concluded that the BCS of Chinese forest increased from 7342 to 11,030 Tg C, and the annual biomass C sink will be 99.68 Tg C·year^{-1}. Our estimate is in agreement with the work of Hu et al., who developed a stage-classified matrix model to predict biomass C stocks of China's forests from 2005 to 2050 by using data from China's forest inventories between 1994 and 2008, the results showed that total forest biomass C stock would increase from 6430 Tg C in 2005 to 9970 Tg C (95% confidence interval: 8980–1107 Tg C) in 2050, with an overall net C gain of 78.8 Tg C·year^{-1}(56.7–103.3 Tg C·year^{-1}) [64]. However, our result is similar to Xu et al. [65], who showed that China's forest biomass carbon storage will increase by 7230 Pg C in 2000–2050, with an average carbon sink of 140 Tg C·year^{-1}, and Yao et al. [66], who estimated age-related forest biomass C sequestration to be 6690 Tg C (170 Tg C·year^{-1}) from the 2000s to the 2040s, the total forest biomass in China would increase by 8890–1037 Tg C by the end of 2040s. Besides, the ratio of net growth to gross growth will increase, and the ratio of net loss to gross loss will decrease. Li et al. [67] estimated the regional carbon emissions of forest harvests with the Fifth and Seventh NFI data sets (1994–1998 and 2004–2008) and found that the total biomass carbon loss caused by forest fires, insect pests, timber harvesting, and other human activities was approximately 131 Tg C·year^{-1}. These results may be related to the general law of forests growth but mainly are related to the human demand for wood. Biomass loss is affected by various factors; for example, biomass loss in Russia, Canada, and the western United States is mainly due to changes in forest structure, the impact of fires and pests, and drought stress, respectively.

Carbon sequestration of forests is mainly due to tree growth and area expansion [24]. In addition, Pan et al. [60] suggests that extensive areas of relatively young forests have the potential to continue sequestering C in the future in the absence of accelerated natural disturbance, climate variability, and land use changes. Most of China's forest stands are in the middle and young ages, as shown in Figure 4I. Moreover, the government has paid increasing attention to protecting the ecosystem and has implemented several major projects for afforestation to increase the forest area, indicating that China will have great carbon sequestration potential in the future and will play an important role in mitigating climate warming.

Although the difference equation can be used for rapid, simple, and efficient tree growth estimates, it still has some limitation in forecasting the BCS. For example, (1) the influence of external environmental factors in the equation was regarded as a fixed value k instead of dynamic change; and (2) the model cannot be used to predict the soil carbon, as soil carbon research is also an important aspect of forest C stock and sink studies.

5. Conclusions

This study, which was based on the basic principle of the difference equation and the general law of tree growth and empirical equations, developed and verified a growth difference equation for the main arbor species in China. We found that the parameters of the difference equation for DBH/tree height was less affected by the spatial position, a certain similarity existed between tree species belonging to a single group, and the parameters of different species was significantly different. Besides, the difference equation was used to predict the growth status and BCS of Chinese forests from 2013 to 2050. The results showed that from 2013 to 2050, the BCS of Chinese forests will increase from 7342 to 11,030 Tg C and the annual biomass C sink will reach 99.68 Tg C·year^{-1}, which indicates that Chinese land-surface forest vegetation have important carbon sequestration capabilities.

In a future study, we hope to (1) use data that distribute across the whole study area for the difference equation fitting and do some application, and (2) investigate the increase of volume, biomass and BCS both for the growth of trees and the expansion of forest area. Moreover, (3) a study related to documenting the stand-level characteristics such as age-class distribution, species composition, stand density, basal area, volume, etc. in BCS research, are also recommended to be carried out.

Author Contributions: H.Z., Z.F., P.C. and X.C. conceived and designed the study; H.Z., P.C., X.C. collected the data; H.Z. and X.C. processed the data; H.Z., and P.C. performed the model fitting; H.Z. and Z.F. supported data analysis; and H.Z., Z.F., P.C. and X.C. wrote the main manuscript. All authors contributed in writing and reviewing the paper.

Funding: This research was jointly funded by the National Natural Science Foundation of China (No. U1710123) and the Fundamental Research Funds for the Central Universities (No. 2015ZCQ-LX-01).

Acknowledgments: The authors thank the associate editors and reviewers for helpful comments and suggestion. We also grateful to the Precision Forestry Key Laboratory of Beijing, Beijing Forestry University for providing all needed facilities to accomplish this study.

Conflicts of Interest: The authors declare no conflict of interest.

Appendix A

Table A1. Modeling parameters of Chinese tree species forest stock volume.

Species (Groups)	c_j	b_j	g_j	f_j
Quercus spp.	5.63056×10^{-5}	0.457	1.87350	0.99969
Betula spp.	5.36548×10^{-5}	0.406	1.87113	0.99050
Larix spp.	5.64302×10^{-5}	0.554	1.79286	1.07499
Pinus massoniana Lamb.	6.11955×10^{-5}	0.663	1.86356	0.96431
Pinus yunnanensis	5.82901×10^{-5}	0.527	1.97963	0.90715
Picea asperata Mast	6.18416×10^{-5}	0.516	1.81373	1.03963
Abies fabri (Mast.) Craib	6.59102×10^{-5}	0.489	1.85472	1.00400
Cupressus funebris Endl.	7.45729×10^{-5}	0.531	1.87266	0.91363
Cunninghamia lanceolata	5.84195×10^{-5}	0.610	1.96266	0.89525
Populus L.	5.77279×10^{-5}	0.530	1.92099	0.92660
Pinus tabuliformis Carrière	6.64925×10^{-5}	0.632	1.86556	0.93769
Other species	5.96868×10^{-5}	0.485	1.92063	0.92505

Note: The parameter "Other species" is the average value of other tree species.

Table A2. The Forest Stock—forest biomass conversion relationship model coefficients.

Species (Groups)	p_j	q_j
Quercus spp.	0.96	43.056
Betula spp.	0.82	18.08
Larix spp.	0.92	−12.64
Pinus massoniana Lamb.	0.65	25.761
Pinus yunnanensis	0.71	18.993
Picea asperata Mast	0.48	81.143
Abies fabri (Mast.) Craib	0.53	22.951
Cupressus funebris Endl.	0.54	46.846
Cunninghamia lanceolata	0.53	22.954
Populus L.	0.72	24.932
Pinus tabuliformis Carrière	0.78	13.889
Other species	0.836	18.668

Note: The parameter of *Pinus yunnanensis* was replaced with other pine parameters and the parameter "Other species" is the average value of other tree species.

Table A3. Modeling parameter of Chinese tree species biomass carbon content.

Species (Groups)	r_j (%)
Quercus spp.	48.32
Betula spp.	49.38
Larix spp.	52.59
Pinus massoniana Lamb.	51.44
Pinus yunnanensis	52.81
Picea asperata Mast	51.6
Abies fabri (Mast.) Craib	50.5
Cupressus funebris Endl.	52.11
Cunninghamia lanceolata	53.65
Populus L.	49.56
Pinus tabuliformis Carrière	53.14
Other species	51.39

Note: The parameter "Other species" is the average value of other tree species.

Table A4. Fitting results for the Richards (1959) equation for different species.

Species (Groups)	DBH				Height			
	A	c	r	R^2	A	c	r	R^2
Pinus massoniana Lamb.	46.837	1.689	0.026	0.755	26.515	1.905	0.046	0.89
Abies fabri (Mast.) Craib	32.527	3.545	0.032	0.691	19.553	2.728	0.032	0.669
Platycladus orientalis (L.) Franco	77.883	0.787	0.002	0.857	20.287	0.56	0.004	0.793
Cunninghamia lanceolata	29.314	1.309	0.043	0.592	19.7	1.724	0.073	0.622
Larix gmelinii (Rupr.) Kuzen	30.621	1.604	0.015	0.725	27.879	1.469	0.019	0.864
Larix principis-rupprechtii Mayr	14.322	7.699	0.108	0.558	12.035	5.201	0.104	0.74
Picea asperata Mast	68.147	1.234	0.005	0.519	13.135	1.83	0.025	0.596
Quercus	26.682	1.554	0.018	0.831	13.192	1.347	0.029	0.85
Pinus tabuliformis Carrière	45.718	1.051	0.007	0.629	12.031	1.278	0.027	0.722
Betula platyphylla Suk.	18.882	2.491	0.049	0.764	15.769	1.755	0.048	0.853
Populus davidiana	13.064	4.23	0.09	0.68	10.65	2.765	0.099	0.701
Populus L.	13.755	1.744	0.069	0.319	14.423	1.116	0.045	0.422
Picea likiangensis	93.367	0.98	0.004	0.772	46.196	1.277	0.009	0.855
Pinus yunnanensis	45.416	1.025	0.017	0.743	32.426	1.367	0.03	0.889
Abies georgei Orr	61.518	1.472	0.004	0.854	26.583	1.674	0.007	0.861

Note: The parameter "Other species" is the average value of other tree species.

Table A5. Fitting results for the Logistic (1983) equation for different species.

Species (Groups)	DBH				Height			
	A	**m**	**r**	R^2	**A**	**m**	**r**	R^2
Pinus massoniana Lamb.	39.032	11.043	0.067	0.743	24.372	11.195	0.096	0.876
Abies fabri (Mast.) Craib	29.435	26.181	0.064	0.689	17.496	21.255	0.07	0.664
Platycladus orientalis (L.) Franco	36.559	6.155	0.019	0.836	14.265	3.225	0.023	0.742
Cunninghamia lanceolata	24.994	7.356	0.112	0.58	18.373	8.916	0.146	0.619
Larix gmelinii (Rupr.) Kuzen	26.766	9.469	0.036	0.718	25.262	8.169	0.042	0.85
Larix principis-rupprechtii Mayr	13.503	57.871	0.181	0.563	11.234	41.878	0.188	0.744
Picea asperata Mast	29.932	12.268	0.035	0.489	8.576	21.054	0.097	0.579
Quercus	19.826	10.596	0.056	0.81	11.56	7.323	0.071	0.835
Pinus tabuliformis Carrière	23.739	8.273	0.047	0.59	9.775	9.336	0.086	0.698
Betula platyphylla Suk.	16.204	16.859	0.109	0.754	13.537	11.386	0.116	0.841
Populus davidiana	12.373	26.342	0.155	0.687	10.195	15.103	0.175	0.707
Populus L.	13.301	7.129	0.119	0.319	13.093	5.281	0.104	0.41
Picea likiangensis	60.677	7.267	0.019	0.747	39.296	8.173	0.025	0.837
Pinus yunnanensis	37.445	5.494	0.051	0.728	29.654	6.805	0.065	0.875
Abies georgei Orr	41.049	12.414	0.017	0.848	21.068	13.646	0.02	0.856

Note: The parameter "Other species" is the average value of other tree species.

Table A6. Validation precision of Richards (1959) model for different tree species.

Species (Groups)	DBH				Height			
	Bias (cm)	**MAE (cm)**	**RMSE (cm)**	R^2_{emp}	**Bias (m)**	**MAE (m)**	**RMSE (m)**	R^2_{emp}
Pinus massoniana Lamb.	−2.74	5.369	7.004	0.697	−0.954	2.589	3.304	0.838
Abies fabri (Mast.) Craib	−1.916	6.796	9.318	0.178	−2.086	4.521	5.999	0.248
Platycladus orientalis (L.) Franco	−4.314	4.351	4.974	0.896	−2.365	2.405	2.862	0.683
Cunninghamia lanceolata	0.521	3.886	4.996	0.642	0.197	2.815	3.665	0.668
Larix gmelinii (Rupr.) Kuzen	0.108	3.384	4.395	0.792	−1.273	2.426	3.248	0.828
Larix principis−rupprechtii Mayr	0.165	2.459	3.167	0.663	0.231	1.364	2.153	0.823
Picea asperata Mast	−0.488	2.667	3.159	0.486	−0.039	1.244	1.685	0.704
Quercus	1.502	2.523	3.601	0.761	0.978	1.931	2.801	0.637
Pinus tabuliformis Carritii	0.221	2.707	3.505	0.576	0.702	1.4	1.896	0.679
Betula platyphylla Suk.	0.719	1.589	2.014	0.843	0.521	1.538	2.115	0.745
Populus davidiana	3.933	4.167	6.232	0.395	2.363	3.111	4.219	0.483
Populus L.	−0.55	2.325	2.815	0.616	−1.623	3.224	4.096	0.37
Picea likiangensis	−1.294	7.3	9.383	0.709	−1.092	3.692	5.105	0.828
Pinus yunnanensis	2.52	7.124	8.454	0.581	0.682	3.572	4.575	0.761
Abies georgei Orr	8.054	9.242	13.433	0.409	2.587	3.71	5.334	0.609

Note: The parameter "Other species" is the average value of other tree species.

Table A7. Validation precision of the Logistic (1983) model for different tree species.

Species (Groups)	DBH				Height			
	Bias (cm)	MAE (cm)	RMSE (cm)	$R^2{}_{emp}$	Bias (m)	MAE (m)	RMSE (m)	$R^2{}_{emp}$
Pinus massoniana Lamb.	−2.866	5.555	7.244	0.675	−0.887	2.677	3.383	0.831
Abies fabri (Mast.) Craib	−2.029	6.517	9.23	0.193	−2.118	4.404	5.886	0.276
Platycladus orientalis (L.) Franco	−4.314	4.351	4.974	0.896	−1.976	2.397	2.714	0.715
Cunninghamia lanceolata	0.319	4.008	5.065	0.632	0.123	2.861	3.697	0.663
Larix gmelinii (Rupr.) Kuzen	−0.157	3.594	4.521	0.78	−1.139	2.629	3.275	0.825
Larix principis−rupprechtii Mayr	0.091	2.468	3.176	0.661	0.181	1.367	2.168	0.82
Picea asperata Mast	−0.032	2.749	3.227	0.463	−0.055	1.289	1.701	0.699
Quercus	1.332	2.585	3.614	0.76	0.897	1.959	2.808	0.635
Pinus tabuliformis Carrière	−0.033	2.87	3.639	0.543	0.678	1.478	1.943	0.663
Betula platyphylla Suk.	0.619	1.637	2.051	0.837	0.511	1.566	2.133	0.741
Populus davidiana	4.03	4.233	6.425	0.357	2.366	3.178	4.312	0.459
Populus L.	−1.637	3.254	4.076	0.376	−0.57	2.412	2.855	0.605
Picea likiangensis	−0.523	7.495	9.273	0.716	−1.327	3.981	5.254	0.817
Pinus yunnanensis	2.16	7.012	8.412	0.585	0.646	3.699	4.695	0.749
Abies georgei Orr	7.345	9.059	12.827	0.461	2.709	3.819	5.49	0.586

Note: The parameter "Other species" is the average value of other tree species.

References

1. Laubhann, D.; Sterba, H.; Reinds, G.J.; De Vries, W. The impact of atmospheric deposition and climate on forest growth in European monitoring plots: An individual tree growth model. *For. Ecol. Manag.* **2009**, *258*, 1751–1761. [CrossRef]
2. Zeng, W.; Zhang, L.; Chen, X.; Cheng, Z.; Ma, K.; Li, Z. Construction of compatible and additive individual-tree biomass models forPinustabulaeformis in China. *Can. J. For. Res.* **2017**, *47*, 467–475. [CrossRef]
3. Couture, S.; Reynaud, A. Forest management under fire risk when forest carbon sequestration has value. *Ecol. Econ.* **2011**, *70*, 2002–2011. [CrossRef]
4. Richards, K.R.; Stokes, C. A review of forest carbon sequestration cost studies: A dozen years of research. *Clim. Chang.* **2004**, *63*, 1–48. [CrossRef]
5. Battle, M.; Bender, M.L.; Tans, P.P.; White, J.W.; Ellis, J.T.; Conway, T.; Francey, R.J. Global carbon sinks and their variability inferred from atmospheric O_2 and delta13C. *Science* **2000**, *287*, 2467–2470. [CrossRef] [PubMed]
6. Fei, X.; Song, Q.; Zhang, Y.; Liu, Y.; Sha, L.; Yu, G.; Zhang, L.; Duan, C.; Deng, Y.; Wu, C.; et al. Carbon exchanges and their responses to temperature and precipitation in forest ecosystems in Yunnan, Southwest China. *Sci. Total Environ.* **2018**, *616–617*, 824–840. [CrossRef]
7. Pan, Y.; Birdsey, R.A.; Phillips, O.L.; Jackson, R.B. The Structure, Distribution, and Biomass of the World's Forests. *Ann. Rev. Ecol. Evol. Syst.* **2013**, *44*, 593–622. [CrossRef]
8. Dobbertin, M. Tree growth as indicator of tree vitality and of tree reaction to environmental stress: A review. *Eur. J. For. Res.* **2005**, *124*, 319–333. [CrossRef]
9. Choi, J.; An, H. A Forest Growth Model for the Natural Broadleaved Forests in Northeastern Korea. *Forests* **2016**, *7*, 288. [CrossRef]
10. Condés, S.; Sterba, H. Comparing an individual tree growth model for Pinus halepensis Mill. in the Spanish region of Murcia with yield tables gained from the same area. *Eur. J. For. Res.* **2008**, *127*, 253–261. [CrossRef]
11. Qin, J.; Cao, Q.V. Using disaggregation to link individual-tree and whole-stand growth models. *Can. J. For. Res.* **2006**, *36*, 953–960. [CrossRef]
12. Moreno, P.; Palmas, S.; Escobedo, F.; Cropper, W.; Gezan, S. Individual-Tree Diameter Growth Models for Mixed Nothofagus Second Growth Forests in Southern Chile. *Forests* **2017**, *8*, 506. [CrossRef]
13. Marchi, M. Nonlinear versus linearised model on stand density model fitting and stand density index calculation: Analysis of coefficients estimation via simulation. *J. For. Res.* **2019**, 1–8. [CrossRef]
14. Andreassen, K.; Tomter, S.M. Basal area growth models for individual trees of Norway spruce, Scots pine, birch and other broadleaves in Norway. *For. Ecol. Manag.* **2003**, *180*, 11–24. [CrossRef]

15. Thurnher, C.; Klopf, M.; Hasenauer, H. MOSES—A tree growth simulator for modelling stand response in Central Europe. *Ecol. Model.* **2017**, *352*, 58–76. [CrossRef]
16. Sharkovsky, A.N.; Maistrenko, Y.L.; Romanenko, E.Y. *Difference Equations and Their Applications*; Springer Science & Business Media: Berlin, Germany, 2012; Volume 250.
17. Lakshmikantham, V.; Trigiante, D. *Theory of Difference Equations: Numerical Methods and Applications*; Marcel Dekker: New York, NY, USA, 2002; Volume 251.
18. Agarwal, R.P. *Difference Equations and Inequalities: Theory, Methods, and Applications*; CRC Press: Boca Raton, FL, USA, 2000.
19. Aloqeili, M. Dynamics of a rational difference equation. *Appl. Math. Comput.* **2006**, *176*, 768–774. [CrossRef]
20. Kelley, W.G.; Peterson, A.C. *Difference Equations: An Introduction with Applications*; Academic Press: Cambridge, MA, USA, 2001.
21. Deeba, E.Y.; Korvin, A.D.; Koh, E.L. A fuzzy difference equation with an application. *J. Differ. Equ. Appl.* **1996**, *2*, 365–374. [CrossRef]
22. Tomé, J.; Tomé, M.; Barreiro, S.; Paulo, J.A. Age-independent difference equations for modelling tree and stand growth. *Can. J. For. Res.* **2006**, *36*, 1621–1630. [CrossRef]
23. Fang, J.; Tang, Y.; Son, Y. Why are East Asian ecosystems important for carbon cycle research? *Sci. China Life Sci.* **2010**, *53*, 753–756. [CrossRef]
24. Li, P.; Zhu, J.; Hu, H.; Guo, Z.; Pan, Y.; Birdsey, R.; Fang, J. The relative contributions of forest growth and areal expansion to forest biomass carbon sinks in China. *Biogeosci. Discuss.* **2015**, *12*, 9587–9612. [CrossRef]
25. Meng, Q.; Cieszewski, C.J.; Strub, M.R.; Borders, B.E. Spatial regression modeling of tree height–diameter relationships. *Can. J. For. Res.* **2009**, *39*, 2283–2293. [CrossRef]
26. Saud, P.; Lynch, T.B.; Wilson, D.S.; Stewart, J.; Guldin, J.M.; Heinemann, B.; Holeman, R.; Wilson, D.; Anderson, K. Influence of weather and climate variables on the basal area growth of individual shortleaf pine trees. In Proceedings of the 17th Biennial Southern Silvicultural Research Conference, Shreveport, LA, USA, 5–7 March 2013; Holley, A.G., Connor, K.F., Eds.; US Department of Agriculture, Forest Service, Southern Research Station: Asheville, NC, USA, 2015; pp. 406–408.
27. Foster, J.R.; Finley, A.O.; D'Amato, A.W.; Bradford, J.B.; Banerjee, S. Predicting tree biomass growth in the temperate-boreal ecotone: Is tree size, age, competition, or climate response most important? *Glob. Chang. Biol.* **2016**, *22*, 2138–2151. [CrossRef] [PubMed]
28. Zhang, L.; Jiang, Y.; Zhao, S.; Jiao, L.; Wen, Y. Relationships between Tree Age and Climate Sensitivity of Radial Growth in Different Drought Conditions of Qilian Mountains, Northwestern China. *Forests* **2018**, *9*, 135. [CrossRef]
29. Meng, X.Y. *Dendrometria*; China Forestry Publishing House: Beijing, China, 1996. (Chinese with English Abstract)
30. Martin, T.M.; Harten, P.; Young, D.M.; Muratov, E.N.; Golbraikh, A.; Zhu, H.; Tropsha, A. Does Rational Selection of Training and Test Sets Improve the Outcome of QSAR Modeling? *J. Chem. Inf. Model.* **2012**, *52*, 2570–2578. [CrossRef] [PubMed]
31. Zeng, W.; Tomppo, E.; Healey, S.P.; Gadow, K.V. The national forest inventory in China: History-results-international context. *For. Ecosyst.* **2015**, *2*, 23. [CrossRef]
32. Kulenović, M.; Ladas, G.; Prokup, N.R. A rational difference equation. *Comput. Math. Appl.* **2001**, *41*, 671–678. [CrossRef]
33. Liu, M.; Feng, Z.; Ma, C.; Yang, L. Influencing factors and growth state classification of a natural Metasequoia population. *J. For. Res.* **2019**, *30*, 337–345. [CrossRef]
34. Qiu, Z.; Feng, Z.; Wang, M.; Li, Z.; Lu, C. Application of UAV Photogrammetric System for Monitoring Ancient Tree Communities in Beijing. *Forests* **2018**, *9*, 735. [CrossRef]
35. Zhang, C.; Ju, W.; Chen, J.M.; Zan, M.; Li, D.; Zhou, Y.; Wang, X. China's forest biomass carbon sink based on seven inventories from 1973 to 2008. *Clim. Chang.* **2013**, *118*, 933–948. [CrossRef]
36. Fang, J.; Chen, A.; Peng, C.; Zhao, S.; Ci, L. Changes in Forest Biomass Carbon Storage in China between 1949 and 1998. *Science* **2001**, *292*, 2320–2322. [CrossRef]
37. Cheng, W. Design and Implementation of the Basic Platform of Forest Resources Management. Master's Thesis, Beijing Forestry University, Beijing, China, 2018. (Chinese with English Abstract).
38. Fang, J.; Guo, Z.; Piao, S.; Chen, A. Terrestrial vegetation carbon sinks in China, 1981–2000. *Sci. China Ser. D Earth Sci.* **2007**, *50*, 1341–1350. [CrossRef]

39. Qiu, Z. Measurement and Statistics of Land-Surface Forest Vegetation Carbon Sink in China. Ph.D. Thesis, Beijing Forestry University, Beijing, China, 2019. (Chinese with English Abstract).
40. Saud, P.; Wang, J.; Lin, W.; Sharma, B.D.; Hartley, D.S. A life cycle analysis of forest carbon balance and carbon emissions of timber harvesting in West Virginia. *Wood Fiber Sci.* **2013**, *45*, 250–267.
41. Huang, C.; Zhang, J.; Yang, W.; Tang, X.; Zhang, G. Dynamics on forest carbon stock in Sichuan Province and Chongqing City. *Acta Ecol. Sin.* **2008**, *28*, 966–975, (Chinese with English Abstract).
42. Huang, S.; Yang, Y.; Wang, Y.; Amaro, A.; Reed, D.; Soares, P. A critical look at procedures for validating growth and yield models, Modelling forest systems. Presented at the Workshop on the Interface between Reality, Modelling and the Parameter Estimation Processes, Sesimbra, Portugal, 2–5 June 2002.
43. Zeng, W.; Duo, H.; Lei, X.; Chen, X.; Wang, X.; Pu, Y.; Zou, W. Individual tree biomass equations and growth models sensitive to climate variables for Larix spp. in China. *Eur. J. For. Res.* **2017**, *136*, 233–249. [CrossRef]
44. Cai, D.; Delcher, A.; Kao, B.; Kasif, S. Modeling splice sites with Bayes networks. *Bioinformatics* **2000**, *16*, 152–158. [CrossRef] [PubMed]
45. Han, Y.; Wu, B.; Wang, K.; Guo, E.; Dong, C.; Wang, Z. Individual-tree form growth models of visualization simulation for managed Larix principis-rupprechtii plantation. *Comput. Electron. Agric.* **2016**, *123*, 341–350. [CrossRef]
46. Saud, P.; Lynch, T.B.; K.C, A.; Guldin, J.M. Using quadratic mean diameter and relative spacing index to enhance height–diameter and crown ratio models fitted to longitudinal data. *Forestry* **2016**, *89*, 215–229. [CrossRef]
47. Scolforo, H.F.; Scolforo, J.R.S.; Thiersch, C.R.; Thiersch, M.F.; McTague, J.P.; Burkhart, H.; Ferraz Filho, A.C.; de Mello, J.M.; Roise, J. A new model of tropical tree diameter growth rate and its application to identify fast-growing native tree species. *For. Ecol. Manag.* **2017**, *400*, 578–586. [CrossRef]
48. Zhang, Y.; Song, C. Impacts of Afforestation, Deforestation, and Reforestation on Forest Cover in China from 1949 to 2003. *J. For.* **2006**, *104*, 383.
49. Webster, C.R.; Lorimer, C.G. Minimum opening sizes for canopy recruitment of midtolerant tree species: A retrospective approach. *Ecol. Appl.* **2005**, *15*, 1245–1262. [CrossRef]
50. Kozak, A.; Kozak, R. Does cross validation provide additional information in the evaluation of regression models? *Can. J. For. Res.* **2003**, *33*, 976–987. [CrossRef]
51. Mehtatalo, L.; De-Miguel, S.; Gregoire, T.G. Modeling height-diameter curves for prediction. *Can. J. For. Res.* **2015**, *45*, 826–837. [CrossRef]
52. Gollob, C.; Ritter, T.; Vospernik, S.; Wassermann, C.; Nothdurft, A. A Flexible Height–Diameter Model for Tree Height Imputation on Forest Inventory Sample Plots Using Repeated Measures from the Past. *Forests* **2018**, *9*, 368. [CrossRef]
53. Zhao, D.H.; Borders, B.; Wilson, M. Individual-tree diameter growth and mortality models for bottomland mixed-species hardwood stands in the lower Mississippi alluvial valley. *For. Ecol. Manag.* **2004**, *199*, 307–322. [CrossRef]
54. Schliep, E.M.; Dong, T.Q.; Gelfand, A.E.; Li, F. Modeling individual tree growth by fusing diameter tape and increment core data. *Environmetrics* **2014**, *25*, 610–620. [CrossRef]
55. Lhotka, J.M.; Loewenstein, E.F. An individual-tree diameter growth model for managed uneven-aged oak-shortleaf pine stands in the Ozark Highlands of Missouri, USA. *For. Ecol. Manag.* **2011**, *261*, 770–778. [CrossRef]
56. Kiviste, K.; Kiviste, A. Algebraic Difference Equations of Stand Height, Diameter, and Volume Depending on Stand Age and Site Factors for Estonian State Forests. *Math. Comput. For. Nat. Resour. Sci. MCFNS* **2009**, *1*, 67–77.
57. Jiang, X.; Huang, J.; Cheng, J.; Dawson, A.; Stadt, K.J.; Comeau, P.G.; Chen, H.Y.H. Interspecific variation in growth responses to tree size, competition and climate of western Canadian boreal mixed forests. *Sci. Total Environ.* **2018**, *631–632*, 1070–1078. [CrossRef]
58. Jackson, S.T.; Betancourt, J.L.; Booth, R.K.; Gray, S.T. Ecology and the ratchet of events: Climate variability, niche dimensions, and species distributions. *Proc. Natl. Acad. Sci. USA* **2009**, *1062*, 19685–19692. [CrossRef]
59. Stephenson, N.L.; Das, A.J.; Condit, R.; Russo, S.E.; Baker, P.J.; Beckman, N.G.; Coomes, D.A.; Lines, E.R.; Morris, W.K.; Rueger, N.; et al. Rate of tree carbon accumulation increases continuously with tree size. *Nature* **2014**, *507*, 90. [CrossRef]

60. Pan, Y.; Birdsey, R.A.; Fang, J.; Houghton, R.; Kauppi, P.E.; Kurz, W.A.; Phillips, O.L.; Shvidenko, A.; Lewis, S.L.; Canadell, J.G.; et al. A Large and Persistent Carbon Sink in the World's Forests. *Science* **2011**, *333*, 988–993. [CrossRef] [PubMed]
61. Corlett, R.T. The Impacts of Droughts in Tropical Forests. *Trends Plant. Sci.* **2016**, *21*, 584–593. [CrossRef] [PubMed]
62. Pan, Y.D.; Luo, T.X.; Birdsey, R.; Hom, J.; Melillo, J. New estimates of carbon storage and sequestration in China's forests: Effects of age-class and method on inventory-based carbon estimation. *Clim. Chang.* **2004**, *67*, 211–236. [CrossRef]
63. Guo, Z.; Fang, J.; Pan, Y.; Birdsey, R. Inventory-based estimates of forest biomass carbon stocks in China: A comparison of three methods. *For. Ecol. Manag.* **2010**, *259*, 1225–1231. [CrossRef]
64. Hu, H.; Wang, S.; Guo, Z.; Xu, B.; Fang, J. The stage-classified matrix models project a significant increase in biomass carbon stocks in China's forests between 2005 and 2050. *Sci. Rep.* **2015**, *5*, 11203. [CrossRef] [PubMed]
65. Xu, B.; Guo, Z.; Piao, S.; Fang, J. Biomass carbon stocks in China's forests between 2000 and 2050: A prediction based on forest biomass-age relationships. *Sci. China Life Sci.* **2010**, *53*, 776–783. [CrossRef]
66. Yao, Y.; Piao, S.; Wang, T. Future biomass carbon sequestration capacity of Chinese forests. *Sci. Bull.* **2018**, *63*, 1108–1117. [CrossRef]
67. Lai, L.; Huang, X.; Yang, H.; Chuai, X.; Zhang, M.; Zhong, T.; Chen, Z.; Chen, Y.; Wang, X.; Thompson, J.R. Carbon emissions from land-use change and management in China between 1990 and 2010. *Sci. Adv.* **2016**, *2*, e1601063. [CrossRef]